

Signatures of interband scattering in spectroscopic experiments on MgB_2

C. P. Moca and B. Jankó

Material Science Division, Argonne National Laboratory, Argonne, Illinois, 60439
Department of Physics, University of Notre Dame, Notre Dame, Indiana, 46556

Within a two-band, strong coupling model we analyze *SIS*-tunneling conductance, Raman scattering and optical conductivity measured on MgB_2 samples. We find that features observed in tunneling and Raman spectroscopy at intermediate energies $\omega = \Delta_\sigma + \Delta_\pi \simeq 8 \div 10 meV$ can be consistently explained when incoherent scattering between σ and π band is considered. We calculate the optical conductivity and find that strong coupling effects are important for explaining the presently available data, and predict the location and magnitude of interband scattering features for this spectroscopic probe as well.

PACS numbers: 63.20.Kr, 74.20.-z, 74.25.-q

Introduction. The discovery of superconductivity in MgB_2 with a critical temperature $T_C = 39K$ [1] has initiated intense research efforts on elucidating the properties of this surprisingly simple compound. The main reason behind the relatively high transition temperature is still unknown. However, there is a growing consensus that strong electron-phonon interaction [2] is responsible for superconductivity in MgB_2 . The large isotope effect measured by Bud'ko *et al.* [3] for boron ($\alpha = 0.26 \pm 0.03$) clearly shows that phonons associated with boron vibrations play a significant role in superconductivity in this compound. Tunneling and point contact spectroscopy experiments [4, 5, 6, 7, 8, 9] reveal a distribution of energy gap $2\Delta(0)/T_C$ between 1.1 and 4.5. Recent experiments of Giubileo *et al.* [10] pointed the presence of two gaps. Evidence of two gaps were found also in the specific heat [11] and recently in Raman scattering experiments [12].

According to Liu *et al.* [13] the four Fermi surface sheets in MgB_2 can be grouped into quasi two-dimensional σ bands and three dimensional π bands, and the normal and superconducting properties of MgB_2 can be described by an effective two-band model. Within this model they calculated the coupling constants and energy gap ratios in the weak coupling regime. Later Golubov *et al.* [14] provided the two-band decomposition of the superconducting Eliashberg functions $\alpha^2 F_{ij}(\omega)$ (where i and j denote σ and π bands), which describe the electron-phonon coupling in MgB_2 as function of frequency. While electron-phonon interaction was clearly investigated in large spectrum of approximations, the role of scattering between the bands was not analyzed in detail.

We turn our attention to the theory of spectroscopic properties of MgB_2 because, similarly to the situation in cuprate superconductors, the most severe constraints on theoretical models are imposed by spectroscopic measurements. In fact, the aim of this paper is to point out that a *simultaneous* explanation of the main features in *SIS* tunnel spectroscopy [9] and Raman scattering [12] can only be done if one allows for the existence of inco-

herent (momentum non-conserving) single-particle scattering events between. We have also analyzed recent optical conductivity results [18]. We find, as shown in detail below, that agreement between theory and experiment is substantially improved over the weak-coupling analysis by considering strong coupling effects alone. We have also calculated the effect of incoherent interband scattering on such measurements. While the presently available data does not allow us to firmly conclude, that there is evidence for incoherent interband scattering in the optical conductivity data as well, it does not contradict the presence of the process either. We nevertheless present our predictions for optical conductivity in the presence of interband scattering, since we believe that our predictions for this probe will be useful in analyzing future, more accurate measurements.

Theoretical Model. We will adopt a two-band Eliashberg scheme to calculate the various spectroscopic quantities. The weak coupling version of the model for two-band superconductivity was originally proposed by Suhl, Matthias and Walker [15]. However, due to the lack of a genuine two-band superconductor at that time, interest in this model gradually decreased. More recently, the Suhl-Matthias-Walker model was revived and applied to cuprates by Kresin [16]. We have used a similar model [17] to calculate the penetration depth in MgB_2 , and we are now applying this framework to derive the spectroscopic properties as well. The starting point of our analysis is the two-band Hamiltonian $\mathcal{H} = \mathcal{H}_0 + \mathcal{H}_I + \mathcal{H}_{i-b}$. Here \mathcal{H}_0 is describing the free electrons,

$$\mathcal{H}_0 = \sum_{\mathbf{k}, \sigma} \varepsilon_{\mathbf{k}} c_{\mathbf{k}\sigma}^+ c_{\mathbf{k}\sigma} + \sum_{\mathbf{k}, \sigma} \xi_{\mathbf{k}} d_{\mathbf{k}\sigma}^+ d_{\mathbf{k}\sigma} + \sum_{\mathbf{q}} \omega_{\mathbf{q}} b_{\mathbf{q}}^+ b_{\mathbf{q}}. \quad (1)$$

In the above expression $c_{\mathbf{k}\sigma}^+$ ($c_{\mathbf{k}\sigma}$) creates (annihilates) electrons in σ band and $d_{\mathbf{k}\sigma}^+$ ($d_{\mathbf{k}\sigma}$) are similar operators acting in π band. The last term describes the non-interacting phonons with the dispersion given by $\omega_{\mathbf{q}}$. The second term in the Hamiltonian, \mathcal{H}_I corresponds to the

interaction of the conduction electrons with the phonons,

$$\begin{aligned} \mathcal{H}_I &= \sum_{\mathbf{k}, \mathbf{q}, \sigma} V_{\sigma\sigma}(\mathbf{k}, \mathbf{q}) c_{\mathbf{k}+\mathbf{q}\sigma}^+ c_{\mathbf{k}\sigma} (b_{\mathbf{q}} + b_{-\mathbf{q}}^+) \\ &+ \sum_{\mathbf{k}, \mathbf{q}, \sigma} V_{\pi\pi}(\mathbf{k}, \mathbf{q}) d_{\mathbf{k}+\mathbf{q}\sigma}^+ d_{\mathbf{k}\sigma} (b_{\mathbf{q}} + b_{-\mathbf{q}}^+) \quad (2) \\ &+ \sum_{\mathbf{k}, \mathbf{q}, \sigma} V_{\sigma\pi}(\mathbf{k}, \mathbf{q}) \left[c_{\mathbf{k}+\mathbf{q}\sigma}^+ d_{\mathbf{k}\sigma} (b_{\mathbf{q}} + b_{-\mathbf{q}}^+) + h.c. \right] \quad (3) \end{aligned}$$

Finally we introduce a new term \mathcal{H}_{i-b} to account for the *incoherent (momentum non-conserving) interband scattering*

$$\mathcal{H}_{i-b} = \sum_{\mathbf{k}, \sigma} (T_{\mathbf{k}\mathbf{q}} c_{\mathbf{k}\sigma}^+ d_{\mathbf{q}\sigma} + h.c.) \quad (4)$$

. The effect of this last term is the main focus of our study, and we will show below, that it plays an important role in explaining the observed features in spectroscopic measurements.

Our approach is based on the self-consistent solution of the Eliashberg equations corresponding to the Hamiltonian (1-4). Self-consistency is reached on the imaginary axis, and Padé approximation [21] is then used to analytically continue to the real axis. This procedure gives accurately the frequency dependence of the gap functions $\Delta_{\sigma}(\omega)$ and $\Delta_{\pi}(\omega)$ and the renormalization factors $Z_{\sigma}(\omega)$ and $Z_{\pi}(\omega)$. The normal self-energy contribution to the i band due to the direct scattering from and in the j band can be written as $1/(2\tau_{ij})g_j(i\omega_n)$ where $g_i(i\omega_n) = \omega_n/\sqrt{\omega_n^2 + \Delta_i^2(\omega_n)}$ and the anomalous self-energy can be written as $1/(2\tau_{ij})f_j(i\omega_n)$ where $f_i(i\omega_n) = \Delta_i/\sqrt{\omega_n^2 + \Delta_i^2(\omega_n)}$. The structure in $\Delta(\omega)$ usually gives rise to observable variations in the density of states at a frequency comparable with the sum of phonon energy and gap value. However, in MgB_2 the phonon mode most relevant to superconductivity is $E_{2g} \simeq 67meV$, and observation of density of states features at such high energies are difficult to be observed experimentally. For the present calculation we model the phonon density with a lorentzian: $F(\omega) = A/((\omega - \omega_1)^2 + \omega_2^2) - A/(\omega_3^2 + \omega_2^2)$ for $|\omega - \omega_1| < \omega_3$ and zero otherwise. Here the frequency parameters are: $\omega_1 = 67meV$, $\omega_2 = 3.5meV$, and $\omega_3 = 30meV$. With these parameters, and taking a cut-off frequency at $\omega_c = 200meV$, we fix $A = 1.31$ by imposing $\int_0^{\omega_c} F(\omega)d\omega = 1$. The best fit to the experimental temperature dependence of the gap function[22] and with the observed $T_C = 39K$ was found for $\alpha_{\sigma\sigma}^2 = 17.5$, $\alpha_{\pi\pi}^2 = 7.0$, $\alpha_{\sigma\pi}^2 = 1.0$, $\alpha_{\pi\sigma}^2 = 2.0$. The effect of Coulomb pseudopotential have been considered through the renormalized parameters $\mu_{ii}^* = 0.1$ and $\mu_{ij}^* = 0$ for $i \neq j$. The effect of cross-band interaction can be analyzed in terms of $\Gamma_{ij} = \tau_{ij}^{-1}$ which directly describe the scattering rate. This is similar with solving the Eliashberg equation for an alloy where similar terms appear due to scattering on

impurities [20]. Throughout of our calculations we have considered that $\Gamma_{ii} = 0$ (no intra-band scattering) and that only $\Gamma_{ij} \neq 0$ for $i \neq j$.

Break Junction Tunneling. We start the comparison to experiment by analyzing the break junction *SIS* tunneling experimental data of Schmidt *et al.* [9]. A careful analysis of the data reveals the presence a dip at a frequency $\omega \sim \Delta_{\sigma} + \Delta_{\pi} \sim 10meV$ and no measurable effects are seen near the frequency corresponding to the larger gap. This suggests that, due to its *3D* nature, only the π band gives a contribution to the tunneling current in break junctions, while the σ band, due to its quasi *2D* nature, has little overall contribution. The electron-phonon interaction alone does not give a satisfactory explanation for the above mentioned feature, and a new term is needed. This term describes incoherent single particle tunneling between bands, and is formally similar to the proximity term first proposed by McMillan [19]. Within this extended Suhl-Matthias-Walker model, the superconductivity in π band can be thought of as being induced by the σ -band. Scattering between bands diminishes the larger gap while the smaller one is enhanced. More importantly, however, self-energy contributions in lowest order in interband scattering will give rise to intermediate states of energies $\Delta_{\sigma} + \Delta_{\pi} \sim 8 - 10meV$, precisely at the voltage where the dip in the tunnel conductance is seen.

In order to study the effect of the direct inter-band interaction we have first calculated the density of states for each band by using the well known relation $N_S^{(i)}(\omega) = N_N^{(i)}(\omega) Re \left((\omega - \Gamma_T) / \sqrt{(\omega - \Gamma_T)^2 - \Delta_i^2(\omega)} \right)$, where $N_S(\omega)$ and $N_N(\omega)$ are the energy dependent density of states of the material in the superconducting and normal state. We have calculated first the superconducting density of states and then using these results we investigate the *SIS* conductance by calculating first the tunneling current by a direct convolution:

$$I_{i,j}(eV) \sim \int_{-\infty}^{+\infty} [n_F(\omega) - n_F(\omega + eV)] N_S^{(i)}(\omega) N_S^{(j)}(\omega + eV) \quad (5)$$

and then taking the derivative as function of bias. In Eq. (5) $n_F(\omega)$ is the Fermi-Dirac function and $N_S^{(i)}(\omega)$ with $i = \pi, \sigma$ is the density of states corresponding to one of the bands. The conductance can be found by differentiating the tunneling current as function of bias and a direct quantitative comparison with the experimental data is possible. Fig. 1 represents the results obtained for the conductance for the π -band together with the experimental data of Schmidt *et al.* [9]. The interband self-energy leads to modification in the structure of the gap function at energies $\omega = \Delta_{\sigma} + \Delta_{\pi}$. Increasing the scattering rates between the bands lead to (*i*) an enhance of the smaller gap corresponding to the π band and to a decreasing of

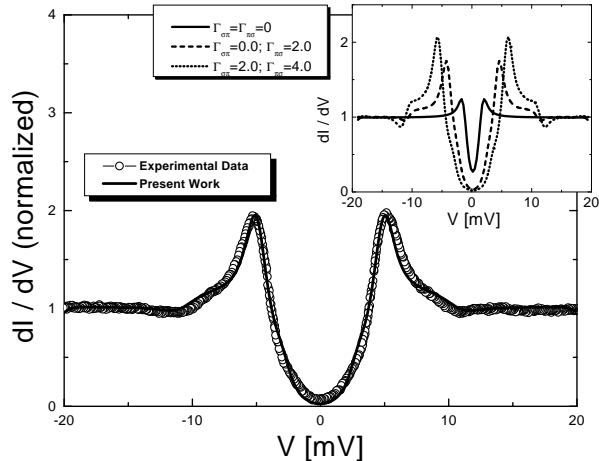


FIG. 1: Results for normalized π -band SIS tunneling conductance (solid line) compared with the experimental data of Schmidt *et al.* [9] (open circle symbols). The scattering rates used in this calculations are $\Gamma_{\pi,\sigma} = 2.5$ and $\Gamma_{\sigma,\pi} = 0.5$. The inset shows the calculated SIS tunneling conductance for different scattering rates.

the σ -band gap; (ii) increasing of the dip feature at the energy $\Delta_\sigma + \Delta_\pi$ in the SIS conductance spectrum. The last effect can be verified experimentally by comparing samples of different impurity concentrations. The presence of impurities will increase such interband scattering processes, and an interesting and somewhat counter-intuitive increase in gap size is therefore expected with the increase of impurity concentration. This would be a qualitative consistency check on our theory.

Raman Spectroscopy. This is the second spectroscopic experiment that we analyze in the same theoretical framework and find an excellent agreement between the experiment and our model. Early Raman experiments performed on MgB_2 were somewhat inconsistent due to differences in sample quality: measurements on poly-crystalline samples[12] reveal the presence of two gaps while single crystal measurements restricted to only ab -plane polarized spectra show only the presence of a one superconducting gap [23]. Recently a more careful analysis resolved this inconsistency and the agreement is that the Raman spectrum does reveal the presence of two bands[24]. We have considered the effect of scattering between the bands when calculating the Raman susceptibility [25] $X(\mathbf{q} \rightarrow 0, \omega)$. The Raman spectrum was calculated separately for each band and then the spectrum was calculated as a weighted sum of contributions from each band. The inset of Fig.2 presents the normalized contributions coming from each band. There is a complete depletion of the Raman spectrum below $2\Delta_i$ for each band and the spectrum has a vertical slope at $2\Delta_i$. The weighting coefficients are 14.61 for π -band and

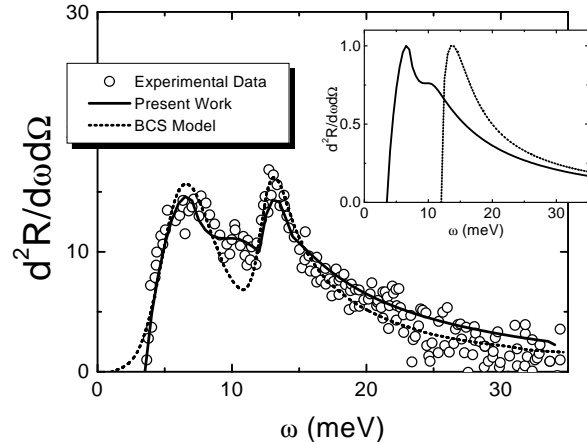


FIG. 2: Calculated Raman spectra at temperature $T = 15K$ (solid line) compared with the experimental data of Chen *et al.* [12] (open symbols). The dotted line represents the two-band BCS like model fit. The scattering rates in these calculations were $\Gamma_{\sigma,\pi} = 0.5$ and $\Gamma_{\pi,\sigma} = 3.0$. The inset presents the normalized results obtained for the Raman spectrum for each band separately.

4.39 for the σ -band leading to a ratio of 3.32 for the contributions of each band (in contrast with the 2.97 ratio obtained in the Suhl-Matthias-Walker model by Chen *et al.*[12]). In our calculations the Raman vertex was calculated for simplicity in the limit $\gamma(\mathbf{p}) = 1$. Even in this limit the effect of scattering between different bands is important, and leads to significant modifications of the spectrum. Our results for the Raman spectrum are presented in Fig.2 and compared to the experimental data of Chen *et al.* [12]. The dashed line is the weak coupling BCS two-band model fit proposed by the same authors. The significant difference between our results and theirs is the presence of the hump at an energy $\omega = \Delta_\sigma + \Delta_\pi$, a feature that theoretically can be obtained by considering only the scattering between the bands, and does not appear in the simple Suhl-Matthias-Walker model. In our calculations the best fit of the experimental data was obtained when $\Gamma_{\sigma,\pi} = 0.5$ and $\Gamma_{\pi,\sigma} = 3.0$. The other parameters used in the calculations are $r \alpha_{\sigma\sigma}^2 = 17.5$, $\alpha_{\pi\pi}^2 = 5.5$, $\alpha_{\sigma\pi}^2 = 1.0$, $\alpha_{\pi\sigma}^2 = 2.0$ and the same values for the Coulomb pseudopotential as in the case of analysis of the tunneling experiment.

Optical Conductivity. The last spectroscopic experiment that we focus on is the optical conductivity, where the importance of the scattering between the bands was analyzed in the framework of Mattis-Bardeen theory [26]. A quantitative comparison with the experimental data on optical conductivity was possible in this case as well, as shown in Fig. 3. One immediate conclusion is already apparent: the overall fit to the experimental data is much

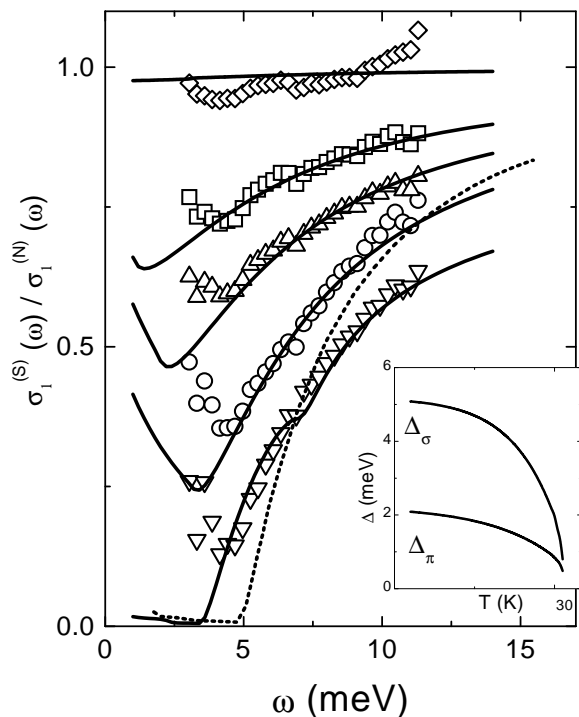


FIG. 3: Real part of conductivity ratio $\sigma_1^{(S)}(\omega)/\sigma_1^{(N)}(\omega)$ for different temperatures (solid lines) from bottom to top $T = 6K, 17.5K, 24K, 27K, 30K$ compared with the experimental data extracted from Ref. [18] (dotted symbols for the same temperatures from bottom to top). The dotted line is the constant gap model for temperature $T=6K$. The scattering rates are $\Gamma_{\sigma,\pi} = 0.5$ and $\Gamma_{\pi,\sigma} = 2.5$. The inset presents the temperature dependence of the gap functions for each band separately.

better in the Eliashberg theory than in the constant gap model. Due to the small critical temperature obtained for the measured sample [18] ($T_C = 30K$) we had to modify the phonon coupling constants in order to obtain the desired critical temperature. Therefore we consider $\alpha_{\sigma\sigma}^2 = 15.5$, $\alpha_{\pi\pi}^2 = 5.0$, $\alpha_{\sigma\pi}^2 = 1.0$, $\alpha_{\pi\sigma}^2 = 2.0$, and for the scattering rates the best fit with the experimental data was obtained for $\Gamma_{\sigma,\pi} = 0.5$ and $\Gamma_{\pi,\sigma} = 2.5$. The small feature appearing in the real part of the optical conductivity at $\omega = \Delta_\sigma + \Delta_\pi \simeq 8meV$ (in this case this energy is smaller due to the smaller critical temperature $\Delta_\pi(T = 0K) = 2.51 meV$, $\Delta_\sigma(T = 0K) = 5.48 meV$), is due to the modifications in the frequency dependence of the gap functions induced by the effect of inter-band scattering in the electronic self-energy. The small feature in the data near this frequency appears to be an extrin-

sic effect [27], and is unlikely to correspond to interband scattering. However, we believe that future experiments will be able to detect the interband structure we predict here.

Conclusions. We have investigated the role of the incoherent inter-band scattering in the framework of two-band strong coupling model. We found results consistent with three experimental measurements. The main results of our work can therefore be summarized as follows: (i) superconductivity in MgB_2 can be well explained in the framework of the two-band model; (ii) The features observed in tunneling spectroscopy, and Raman scattering at energies $\omega = \Delta_\sigma + \Delta_\pi \simeq 8 \div 10meV$ can be consistently explained by considering the incoherent scattering between the bands. While there is no clear feature observed in optical conductivity at this frequency, we predict that such features will eventually be observed, (iii) Overall, the fit to the experimental data is much better if a strong coupling theory is used, rather than a two-band, weak coupling, constant gap model. [9].

Acknowledgments. We are especially indebted to Drs. H. Schmidt and M. Carnahan for supplying us with tunneling and optical spectroscopy data, respectively. We wish to thank them as well as Drs. G. Arnold, G. W. Crabtree, K. Gray, M. Iavarone, W.-K. Kwok, G. Karapetrov, A. Koshelev, J. Orenstein, and J. Zasadzinski for useful discussions.

-
- [1] J. Nagamatsu, N. Nakagawa, T. Muranaka, Y. Zenitani, J. Akimitsu, Nature **410**, 63, (2001).
 - [2] J. Kortus, I. I. Mazin, K. D. Belashchenko, V. P. Antropov, and L. L. Boyer, Phys. Rev. Lett. **86**, 4656, (2001).
 - [3] S. L. Bud'ko, G. Lapertot, C. Petrovic, C. E. Cunningham, N. Anderson, and P. C. Canfield, Phys. Rev. Lett. **86**, 1877, (2001).
 - [4] G. Karapetrov, M. Iavarone, W. K. Kwok, G. W. Crabtree, and D. G. Hinks, Phys. Rev. Lett. **86**, 4374, (2001).
 - [5] G. Rubio-Bollinger, H. Suderow and S. Vieira Phys. Rev. Lett. **86**, 5582, (2001).
 - [6] P. Szabó, P. Samuely, J. Kacmarcik, T. Klein, J. Marcus, D. Fruchart, S. Miraglia, C. Marcenat and A. G. M. Jansen, Phys. Rev. Lett. **87**, 137005, (2001).
 - [7] A. Sharoni, I. Felner and O. Millo, Phys. Rev. **B 63**, 220508, (2001).
 - [8] A. Kohen and G. Deuser, Phys. Rev. **B 64**, 060506(R), (2001).
 - [9] H. Schmidt, J. F. Zasadzinski, K. E. Gray, and D. G. Hinks Phys. Rev. **B 63**, 220504(R) (2001).
 - [10] F. Giubileo, D. Roditchev, W. Sacks, R. Lamy, D. X. Thanh, and J. Klein, S. Miraglia, D. Fruchart, J. Marcus, Ph. Monod Phys. Rev. Lett. **87**, 177008, (2001).
 - [11] F. Bouquet, Y. Wang, R. A. Fisher, D. G. Hinks, J. D. Jorgensen, A. Junod and N. E. Phillips, Phys. Rev. Lett. **87**, 047001 (2001).
 - [12] X. K. Chen, M. J. Konstantinović, J. C. Irwin, D. D. L'Arwie, J. P. Franck, Phys. Rev. Lett. **87**, 157002,

- (2001).
- [13] A. Y. Liu, I. I. Mazin, and J. Kortus, Phys. Rev. Lett. **87**, 08705, (2001).
- [14] A. A. Golubov, J. Kortus, O. V. Dolgov, O. Jepsen, Y. Kong, O. K. Andersen, B. J. Gibson, K. Ah, R. K. Kremer, [cond-mat/0111262](#).
- [15] H. Suhl, B. T. Matthias, and L. R. Walker, Phys. Rev. Lett. **3**, 552, (1959).
- [16] V. Z. Kresin, S. A. Wolf, Phys. Rev. **B 46**, 6458 (1992).
- [17] C. P. Moca, Phys. Rev. **B 65**, 132509, (2002).
- [18] R. A. Kaindl, M. A. Carnahan, J. Orenstein, D. S. Chemla, H. M. Christen, H.-Y. Zhai, M. Pranthaman, D. H. Lowndes, Phys. Rev. Lett. **88**, 027003, (2002).
- [19] W. L. McMillan, Phys. Rev. **175**, 537, (1968).
- [20] J. P. Carbotte Rev. Mod. Phys. **62**, 1027, (1990); F. Marsiglio and J. P. Carbotte [cond-mat/0106143](#); D. J. Scalapino, J. R. Schrieffer, and J. W. Wilkins, Phys. Rev. **148**, 263, (1966).
- [21] H. J. Vidberg and J. W. Serene J. Low. Temp. Phys. **29**, 179, (1977).
- [22] C. Buzea, T. Yamashita, Supercond. Sci. Tech. **14**, R115, (2001) and references therein.
- [23] J. W. Quilty, S. Lee, A. Yamamoto, S. Tajima, Phys. Rev. Lett. **88**, 087001, (2002).
- [24] J. W. Quilty, S. Lee, S. Tajima, A. Yamanaka, [cond-mat/0206506](#).
- [25] C. Jiang, J. P. Carbotte, Phys. Rev. **B 53**, 11868, (1996) and references therein.
- [26] D. C. Mattis, J. Bardeen, Phys. Rev. **111**, 412, (1958).
- [27] M. Carnahan and J. Orenstein (private communication)